Comparative Analysis of Maximum Power Point Tracking Algorithms for Standalone PV System Under Variable Weather Conditions

Aditya Ghatak[1], Tushar Pandit[1], Dharavath Kishan[2,*] and Ravi Raushan[2]

[1]*Electrical and Electronics Engineering, Vellore Institute of Technology, India*
[2]*Electrical and Electronics Engineering, National Institute of Technology, Karnataka, Surathkal, India*
E-mail: kishand@nitk.edu.in
[*]*Corresponding Author*

Received 17 November 2021; Accepted 15 March 2022;
Publication 09 December 2022

Abstract

Renewable energy systems are becoming increasingly predominant in the current scenario, and Photovoltaic (PV) arrays are one of the most widely used renewable energy generation sources. The current-voltage characteristics of PV arrays are non-linear, necessitating the need for supervisory techniques in order to ensure that the array functions at maximum efficiency, which is performed by Maximum Power Point Tracking (MPPT) techniques. These techniques are categorized into classical, intelligent and optimization algorithms. This paper performs a comparative analysis between five different MPPT techniques belonging to these categories – Perturb and Observe (P&O), Incremental Conductance (IC), Fuzzy Logic Control (FLC), Particle Swarm Optimization (PSO) and Cuckoo Search Algorithm (CSA). A standalone PV system interfaced with a Boost converter is simulated on

Distributed Generation & Alternative Energy Journal, Vol. 38_1, 215–248.
doi: 10.13052/dgaej2156-3306.38110

MATLAB Simulink for the performance evaluation of the MPPT techniques. Solar energy is extremely susceptible to changes in local weather conditions, mainly variations in solar insolation levels. The designed system is tested against a varying insolation profile in order to examine the robustness of the MPPT techniques, with their operation efficiencies showcased.

Keywords: Cuckoo search, fuzzy logic, incremental conductance, maximum power point tracking, particle swarm optimization, perturb and observe, photovoltaic.

1 Introduction

The need for renewable resources in the current times are increasing every day and one such important source is solar energy. Solar energy is clean, infinite and free of cost. Photovoltaic (PV) systems are used to tap this energy and convert it to a usable form. [1] PV systems usually comprises of a boost converter which is controlled by a MPPT system to ensure its operation at maximum power at various load conditions. [2] PV systems suffers from two major drawbacks: the electricity generated fluctuates with the weather conditions and the conversion factor from solar energy to the generated electricity is very low (9%–17%) [3].

[4] MPPT helps in the optimization of output PV power to deliver it to the grid, load or an energy storage device. It ensures that even during changing weather conditions, the output PV power will always be maximum. Usage of MPPT helps in reducing the electricity generation cost of the PV panel. Classical MPPT techniques have undergone numerous modifications in increase their operational efficiencies. Perturb and Observe method is one of the most widely used algorithm because of its simplicity and ease of implementation. [5] discusses about a modified P&O system with implementation of rapidly-varying solar irradiation used for the tracking of changing irradiation levels. [6] proposes an improved P&O method using a unique search space algorithm which confines the P-V curve area to 10% near the MPP for optimal operation. [7] implements a checking methodology in a modified P&O algorithm to increase the accuracy of the system for the tracking of point with maximum power in the P-V curve of the PV system. [8] introduces an improved variable step P&O algorithm for a PV system interfaced with the grid-tied system for optimum and quick tracking of MPP, which segments the area of operation of the PV array into 4 sections.

Incremental conductance is a widely used strategy for MPPT, which has undergone several modifications for increasing its operational efficiency. [9] addresses the confusions faced by the algorithm during rapidly changing insolation, and proposes a modification that focuses on recognizing the wrong step change in order to increase the overall efficiency of the algorithm. The results are simulated, and deployed on a microcontroller-controlled hardware setup. [10] proposes a genetic algorithm based Proportional Integral Derivative (PID) controller in order to foresee the variation in step size, and compares the results against the traditional P&O algorithm. [11] proposes a fractional order based modified PID control mechanism for traditional IC based MPPTs in order to obtain faster a convergence time. [12] proposes two subtle modifications to the traditional IC algorithm – a scaling factor that undergoes autonomous variation and an algorithm for slope variation that removes the need for manual tuning.

The reduced effectiveness of classical techniques during unstable weather conditions has resulted in the development of several intelligent MPPT techniques. [13] discusses a modified fuzzy control logic implementing a neural algorithm for the determination of maximum power point with irregular perturbations based on the condition of PV. Numerical simulations are performed indicating its various advantages. [14] design of a new MPPT system based on fuzzy logic control is discussed. An improved MPP tracking is proposed using "antecedent-consequent adaptive" technique. It showcases a faster and even-levelled controller which uses a unique light membership function procedure where these functions are tuned up coherently. [15] introduces an improved MPPT algorithm utilizing a modified P&O system with fuzzy logic implementation for enhancing the PV current output along with the predictive model for the current controller. The algorithm is deployed with a minimum set of rules in order to lower the calculative work. [16] presents a MPPT algorithm using an improved Hill Climbing methodology with fuzzy logic control for generation of duty cycle. The FLC provides robustness to the system by improving its convergence rate and reducing its variance near the MPP.

Various evolutionary optimization techniques which mimic the efficient processes in nature have been used to increase the operational efficiencies MPPT techniques during rapidly changing weather conditions. [17] uses the PSO algorithm in order to optimize the input membership function for a fuzzy logic based MPPT system, and compares the results of the modified algorithm against traditional techniques. [18] combines the PSO based MPPT

with an overall distribution based MPPT to propose a hybrid model that analyzes the areas under the global MPPs in order to increase operational efficiencies. [19] proposes a modified PSO MPPT technique which depends on partitioning of the converter duty ratio into two different segments for the purpose of search optimization. [20] incorporates the SLFA algorithm with the traditional PSO algorithm in order to make the process of searching for the global MPP faster, and compares the modified technique with the traditional MPPT, highlighting a 33% increase in operational efficiency.

[21] proposes a unique MPPT algorithm that combines the Cuckoo Search methodology along with the Golden Section Search algorithm in order to overcome the issues of time taken to trace the MPP and provide higher accuracy than the base model. This method is verified by evaluating it with numerous Partial shading scenarios and improvements in all these cases were observed. [22] discusses about the problems presented by partial shading (PS) of PV and thus proposes a technique to extract maximum power from the PV panel using biological intelligence CS methodology by splitting the two partial shading patterns. [23] reviews the Cuckoo Search methodology for tracking of maximum power point of PV and compares the CS algorithm with other MPPT strategies such as the Neural Network Method and PSO, reaching the conclusion that Cuckoo Search provides better tracing of MPP of the PV with minimum power losses to the PV system.

This paper performs a comprehensive comparison between the performance of five different MPPT techniques under changing solar insolation levels. Section 2 highlights the PV system modelled in MATLAB Simulink for investigating the performances of the different MPPT algorithms. Section 3 gives an outline of each of the five algorithms used and describes the methodologies for their execution – Perturb and Observe, Incremental Conductance, Fuzzy Logic, Particle Swarm Optimization and Cuckoo Search Algorithm. The results are shown and discussed in Section 4, followed by concluding remarks in Section 5.

2 Modelling of PV System

Figure 1 shows the equivalent circuit of a PV array. The parallel shunt resistance R_{sh} represents the leakage resistance, whereas the series resistance R_s represents the resistance of the semiconductor, as well as that between the cell and its leads. The model equation is represented by Equation (1). Table 1 highlights the specifications of the PV system at standard conditions with

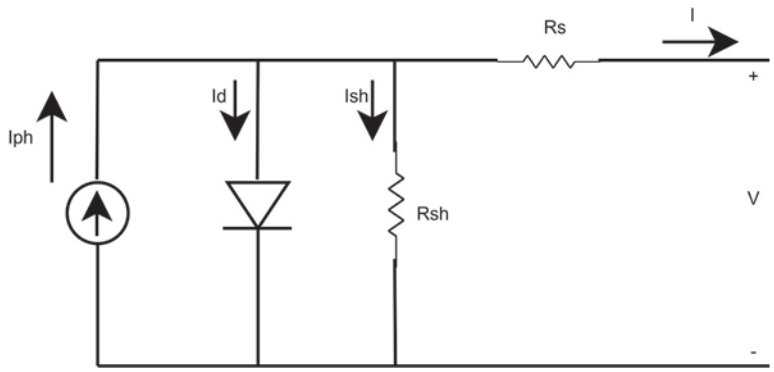

Figure 1 Equivalent circuit of PV array.

Table 1 Specifications of PV module

Parameter	Specifications
Maximum Power Point (MPP)	1467 W
Voltage at MPP	30.2 V
Current at MPP	8.1 A
Open circuit voltage	37.2 V
Short circuit current	8.62 A

1000 W/m^2 irradiance.

$$I = I_{ph} - I_o \left(e^{\frac{q(V+IR_s)}{nkT}} - 1 \right) - \frac{V + IR_s}{R_{sh}} \tag{1}$$

where

I_{ph} = Photocurrent
I_o = Diode saturation current
q = Charge of the electron
R_s = Series resistance
R_{sh} = Shunt resistance
I = Output current
V = Output voltage
T = Module temperature

Figure 2(a) and (b) show the current-voltage and power-voltage characteristics of the PV model for different irradiances. Figure 3(a) and (b) show the current-voltage and power-voltage characteristics for different temperatures. A boost converter is utilized for the implementation of MPPT techniques, as shown in Figure 4. For each MPPT algorithm, the duty ratio obtained as

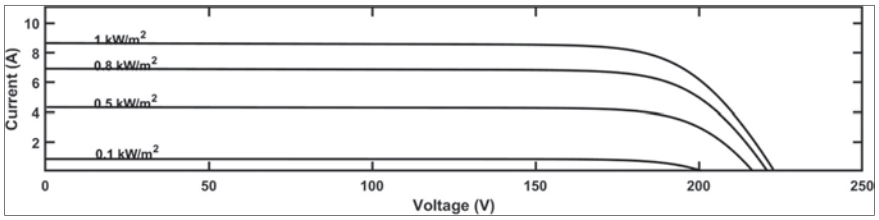

(a)

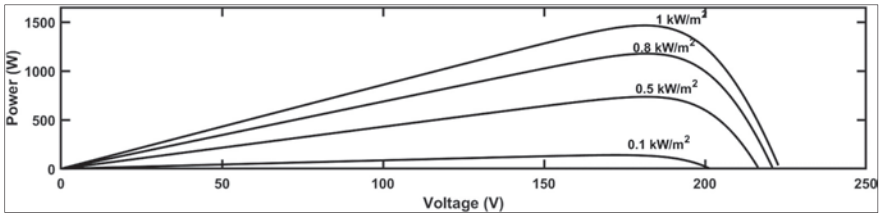

(b)

Figure 2 (a) I-V characteristics of the model for different irradiances (b) P-V characteristics of the model for different irradiances.

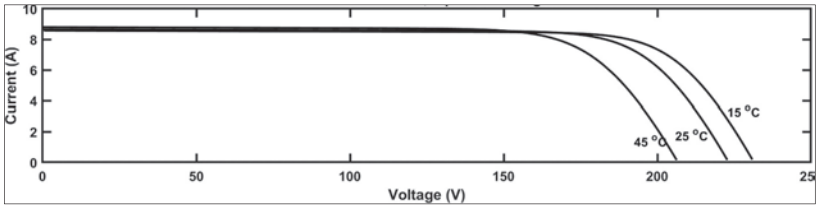

(a)

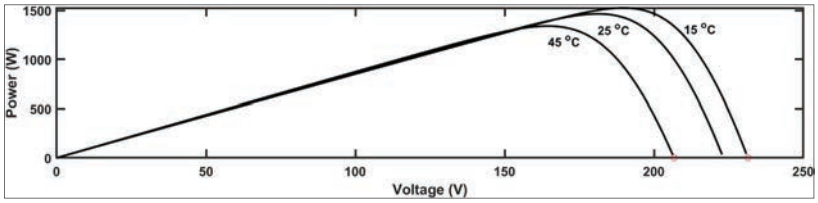

(b)

Figure 3 (a) I-V characteristics of the model for different temperatures (b) P-V characteristics of the model for different temperatures.

Figure 4 Block diagram of MPPT system.

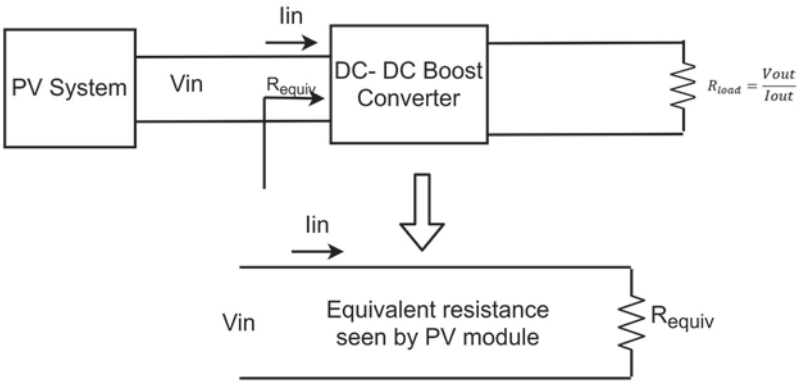

Figure 5 Equivalent circuit of MPPT system.

Table 2 Specifications of boost converter

Parameter	Specification
Switching frequency	10kHz
Current ripple	5%
Voltage ripple	1%
Boost capacitance	500×10^{-6} F
Boost inductance	10^{-3} H

output is used to control the Boost converter. The equivalent circuit of the system is shown in Figure 5. The converter is designed based on Equations (2) and (3). The specifications of the Boost converter are highlighted in Table 2.

$$L_f = \frac{V_i(V_o - V_i)}{f_{sw}\Delta I V_o} \tag{2}$$

$$C_f = \frac{I(V_o - V_i)}{f_{sw}\Delta V V_o} \tag{3}$$

Where

$L_f =$ Inductance
$C_f =$ Capacitance

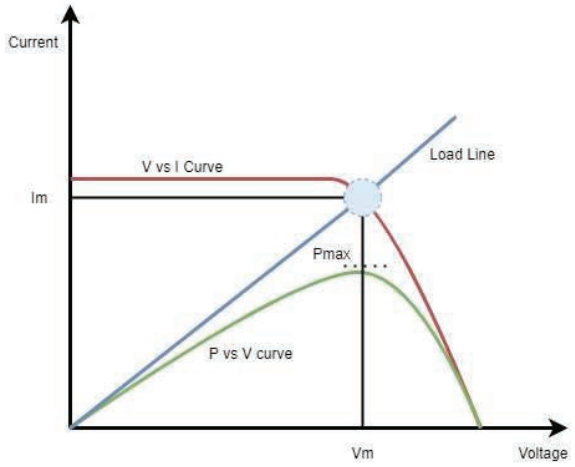

Figure 6 MPPT curve.

$V_o =$ Output voltage
$V_i =$ Input voltage
$f_{sw} =$ Switching frequency
$\Delta I =$ Current ripple

3 Maximum Power Point Tracking Techniques

The purpose of applying MPPT techniques is to make sure that the power delivered by the PV panel to the load is in keeping with the global maximum power point for the P-V curve corresponding to the particular solar insolation level, as shown in Figure 6. The I-V characteristics and the P-V characteristics of the solar PV module are drawn with a load line which is defined as ratio of change in current to change in voltage, and is variable. Despite the variation in the load line, it is desirable to ensure that the system operating point corresponds to the maximum power point of the P-V curve in order to ensure maximum system efficiency.

This paper classifies MPPT techniques into three different categories, as shown in Figure 7 Classical, Intelligent, and Optimization based techniques based on the process of tracking of the global MPP. Classical techniques including Perturb and Observe and Incremental Conductance, which are ware considered for comparison against an intelligent fuzzy logic based MPPT. Evolutionary optimization-based techniques such as Particle Swarm

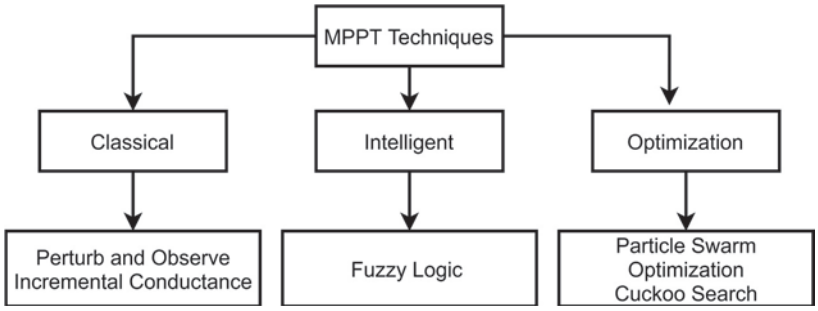

Figure 7 Classification of MPPT techniques.

Optimization (PSO) and Cuckoo Search Algorithm (CSA) are also implemented to account for high operational efficiencies during rapidly changing weather conditions. The choice amongst evolutionary optimization algorithms is made on the basis of high complexity and faster convergence offered by both PSO and CSA techniques.

3.1 Perturb and Observe

The Perturb and Observe (P&O) MPPT technique involves a consistent tracking of the Maximum Power Point (MPP) post applying perturbations to the Boost converter input, and analysing the corresponding power changes.

The flowchart shown in Figure 8 highlights the working of the P&O algorithm. At any given operating point on a P-V characteristics as shown in Figure 9, a small change is given on the operating voltage of a PV array which leads to change in power, represented by dP_{pv}. If this change in power is positive then further perturbation to the voltage (in the corresponding direction of same sign) is given to ensure the operating point reaches the MPP. However, if change in power, dP_{pv}, is negative, it indicates departure of the operating point from the MPP and thus a reversal of the sign of perturbation is done to move the operating point towards MPP. This technique is summarized in Table 3.

Figure 10 shows the P&O MPPT algorithm simulated on MATLAB Simulink. The stepwise execution of the algorithm is mentioned below.

Step I: Measure PV current (I_{pv}) and voltage (V_{pv}).

Step II: Calculate PV power (P_{pv}) from PV current and voltage.

Figure 8 Flowchart of Perturb and Observe MPPT algorithm.

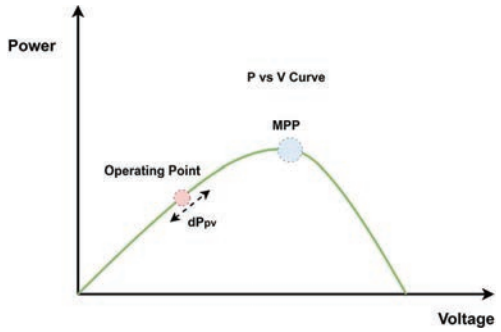

Figure 9 Variation of operating point to reach MPP for P&O MPPT.

Table 3 Perturbation sequence for P&O MPPT

Perturbation	Power Change	Subsequent Perturbation
Positive	Positive	Positive
Positive	Negative	Negative
Negative	Positive	Negative
Negative	Negative	Positive

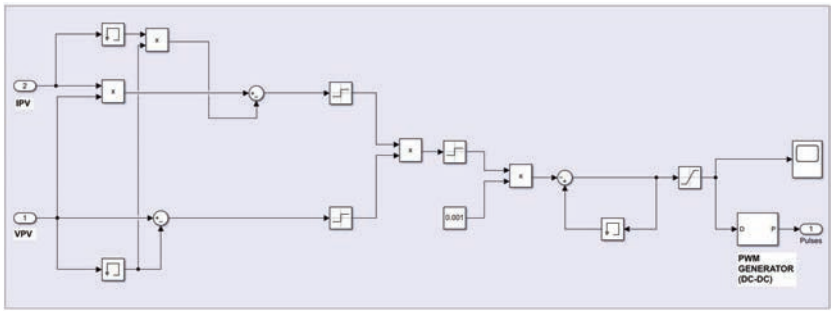

Figure 10 Perturb and Observe MPPT algorithm implemented on Simulink.

Step III: Extract previous values of PV current (I_{pv}(n–1)) and voltage (V_{pv} (n–1)) from memory.

Step IV: Observe the change in power between two consecutive instances to make the following operations:

- If $dP_{pv} > 0$; pass 1
- If $dP_{pv} < 0$; pass -1
- If $dP_{pv} = 0$; pass 0

Step V: Observe the change in voltage between two consecutive instances to make the following operations:

- If $dV_{pv} > 0$; pass 1
- If $dV_{pv} < 0$; pass -1
- If $dV_{pv} = 0$; pass 0

Step VI: The signs obtained from comparisons in Step IV and Step V are then multiplied in order to obtain a net sign, which is then imparted to an incremental duty ratio of 0.001. The increment is either positive, negative, or zero depending on whether the overall duty ratio is to be increased, decreased or kept constant in order to reach the MPP.

Step VII: The duty ratio is limited to permissible values between 0.1 and 0.9, and passed onto a PWM generator in order to provide the gating pulses to the Boost converter.

3.2 Incremental Conductance

The Incremental Conductance (IC) algorithm is based on differentiating the power of PV array with respect to voltage and equating it to zero at MPP.

This is represented in Equation (4).

$$\frac{dP_{pv}}{dV_{pv}} = \frac{d(V_{pv} * I_{pv})}{dV_{pv}} = I_{pv} + V_{pv}\frac{dI_{pv}}{dV_{pv}} \tag{4}$$

At MPP,

$$\frac{dP_{pv}}{dV_{pv}} = 0 \tag{5}$$

$$I_{pv} + V_{pv}\frac{dI_{pv}}{dV_{pv}} = 0 \tag{6}$$

$$\frac{dI_{pv}}{dV_{pv}} = -\frac{I_{pv}}{V_{pv}} \tag{7}$$

where

$\mathrm{I_{PV}}$ = Output current
$\mathrm{V_{PV}}$ = Output voltage
$\frac{\mathrm{dI_{PV}}}{\mathrm{dV_{PV}}}$ = Incremental conductance of PV array
$\frac{\mathrm{I_{PV}}}{\mathrm{V_{PV}}}$ = Instantaneous conductance of PV array

At MPP the quantities shown in Equation (7) will have same magnitude but opposite signs. In case the point of operation is not at the MPP, one of two cases arises:

- *Case I*: Incremental conductance is greater than instantaneous conductance, represented by Equation (8).

$$\frac{dI_{pv}}{dV_{pv}} > -\frac{I_{pv}}{V_{pv}} \tag{8}$$

- *Case II*: Incremental conductance is smaller than instantaneous conductance, represented by Equation (9).

$$\frac{dI_{pv}}{dV_{pv}} < -\frac{I_{pv}}{V_{pv}} \tag{9}$$

Equations (8) and (9) signify the direction at which the perturbation must occur to ensure that point of operation is reaching the MPP. The MPPT algorithm ensures that the point of operation does not waver from MPP unless a change in current is observed which is caused due to variation in irradiance.

The flowchart as shown in Figure 11 provides the overall view of the algorithm. Null values obtained for change in current ($\mathrm{dI_{pv}}$) and change

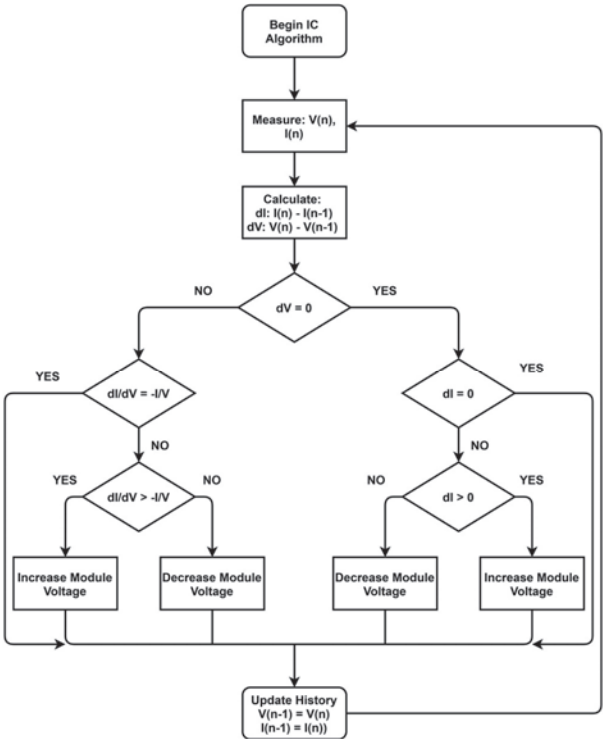

Figure 11 Incremental Conductance MPPT algorithm.

in voltage (dV_{pv}) signify operation in the MPP itself. However, a positive change in current implies an increase in irradiation, prompting the algorithm to increment the voltage in order to shift the current operating point to MPP. Similarly, a negative change in current implies reduced irradiation, and calls for a reduction in the PV voltage for the convergence of the operating point with the MPP. If the current and voltage changes are non-zero then the relation from Equations (7), (8) and (9) are used to determine the point of maximum power.

Figure 12 shows the implementation of Incremental and Conductance algorithm in MATLAB Simulink. The stepwise implementation of the algorithm is mentioned below.

Step I: Measure the PV's output current (I_{pv}) and voltage (V_{pv}).

Step II: Extract the previous values of PV current ($I_{pv}(n–1)$) and voltage ($V_{pv}(n–1)$) from the memory block.

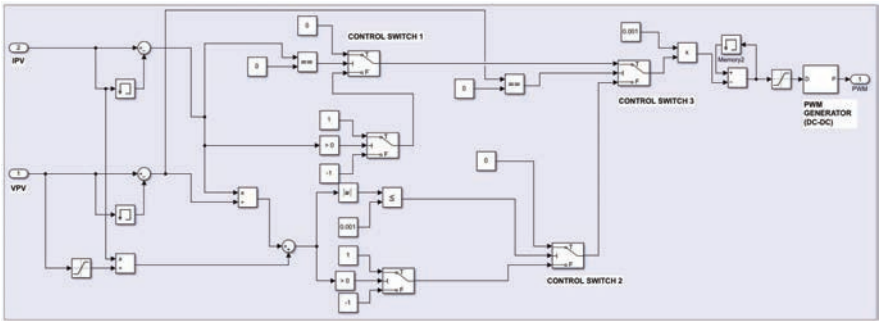

Figure 12 Incremental Conductance MPPT algorithm implemented on Simulink.

Step III: Calculate the change in voltage (dVpv) and current (dI_{pv}) from values obtained from Step I and Step II.

Step IV: Divide dI_{pv} by dV_{pv} to obtain incremental conductance and I_{pv} by V_{pv} to obtain instantaneous conductance.

Step V: If $dV_{pv} = 0$; pass output of Switch 1 from Switch 3
If $dV_{pv} \neq 0$; pass output of Switch 2 from Switch 3
*The output of Switch 1 depends on dI_{pv}.

- If $dI_{pv} = 0$; pass 0
- If $dI_{pv} > 0$; pass 1
- If $dI_{pv} < 0$; pass -1

*The output of switch 2 is dependent on error signal which is defined as $e = \frac{dI_{PV}}{dV_{PV}} + \frac{I_{PV}}{V_{PV}}$.

- If $e > 0$; pass 1
- If $e < 0$; pass -1
- If $|e| <= 0.001$; pass 0

Step VI: The output from Switch 3 is multiplied with 0.001 (incremental duty value) which is then added with the old duty value (obtained through memory block) to achieve a new duty cycle value. This duty cycle is finally passed through a saturation block which is fed to the PWM generator block to obtain the switching pulses for the boost converter.

3.3 Fuzzy Logic Control

Fuzzy Logic Control (FLC) is one of the most profound techniques to determine the maximum power point in the PV system. The advantages that

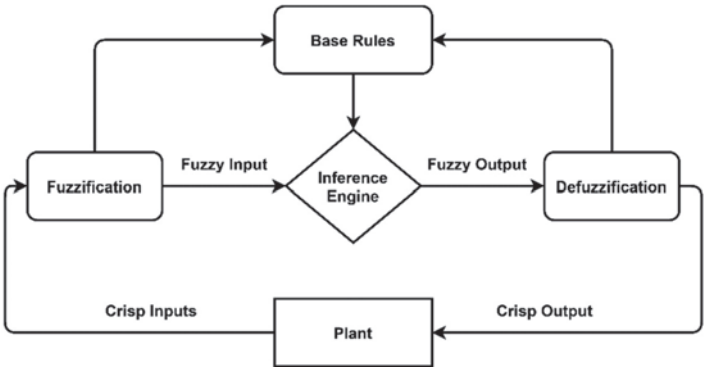

Figure 13 Flowchart of general working of Fuzzy control.

fuzzy logic control offers are robustness of the system, no requirement of a mathematical model and simplicity of design. The working of FLC depends the definition of the membership functions and the rules that guides them. The flowchart of the working of a general fuzzy system is shown in Figure 13.

As shown in Figure 13, the FLC includes three functions – Fuzzification, Interference Engine and Defuzzification. These functions are explained as follows:

(i) Fuzzification: The input variables are first converted to linguistic values that is defined by the membership functions. The FLC takes in two inputs named as error (E) and change in error (ΔE) and gives out an output which is the changing duty cycle (ΔDuty). The inputs at an instant time t are evaluated using the following Equations:

$$E(t) = \frac{P_{pv}(t) - P_{pv}(t-1)}{V_{pv}(t) - V_{pv}(t-1)} = \frac{\Delta P_{pv}}{\Delta V_{pv}} = \frac{\Delta I_{pv}}{\Delta V_{pv}} + \frac{I_{pv}}{V_{pv}} \tag{10}$$

$$\Delta E(t) = E(t) - E(t-1) \tag{11}$$

Where P_{pv}, V_{pv} and I_{pv} are PV's power voltage and current and ΔP_{pv} ΔV_{pv} and ΔI_{pv} are change in PV's power, voltage and current respectively.

The operating point of the PV is then decided by the FLC using these two inputs to the membership functions and the rule-base. E(t) helps in providing information regarding the position of the operating point from the MPP whereas ΔE(t) determines the pace at which the operating point is moving towards or away from the MPP.

- If E(t) > 0, the FLC increases ΔDuty
- If E(t) < 0, the FLC decreases ΔDuty

Table 4 Rule base for fuzzy logic control

E \ ΔE	NB	N_{Low}	Z	P_{Low}	P_{High}
$\mathbf{N}_{High}$	Z	Z	N_{High}	N_{High}	N_{High}
$\mathbf{N}_{Low}$	Z	Z	N_{Low}	N_{Low}	N_{Low}
Z	NS	Z	Z	Z	PS
$\mathbf{P}_{Low}$	P_{Low}	P_{Low}	P_{Low}	Z	Z
$\mathbf{P}_{High}$	P_{High}	P_{High}	P_{High}	Z	Z

(ii) Inference Engine: After determination of E and ΔE these inputs are then undergone transformation to linguistic values with the membership functions defined as shown in Figure. The linguistic values are defined as follows: N_{High} (Negative High), N_{Low} (Negative Low), Z (Zero), P_{Low} (Positive Low), and P_{High} (Positive High). Table 4 shows the 25 rule-base for defining the membership functions. An increase in the rule base size leads to faster system response.

(iii) Defuzzification: The output of FLC is not directly interpreted by the real systems, hence defuzzification is required. In defuzzification, the fuzzy output is transformed to its mathematical equivalent. The signal gets generated which controls the Boost Converter to reach the MPP. Centroid method is used to carry out defuzzification since it provides better results. The crisp output (ΔDuty) obtained from FLC is then enumerated with previous duty cycle whose resultant is then finally passed on to the Boost Converter.

Figure 14 shows the implementation of Fuzzy Logic Control algorithm in MATLAB Simulink. The stepwise implementation of the algorithm is mentioned below.

Step I: Measure the PV's output current $I_{pv}(t)$ and voltage $V_{pv}(t)$.

Step II: Obtain power $P_{pv}(t)$ from current $I_{pv}(t)$ and voltage $V_{pv}(n)$.

Step III: Extract the previous values of PV power $P_{pv}(t–1)$ and voltage $V_{pv}(t–1)$ from memory.

Step IV: Calculate the values ΔP_{pv} and ΔV_{pv} by subtracting the values obtained in *Step II* with *Step III.*

Step V: Obtain error E(n) by dividing ΔP_{pv} by ΔV_{pv}. This indicates the first input to the fuzzy logic controller.

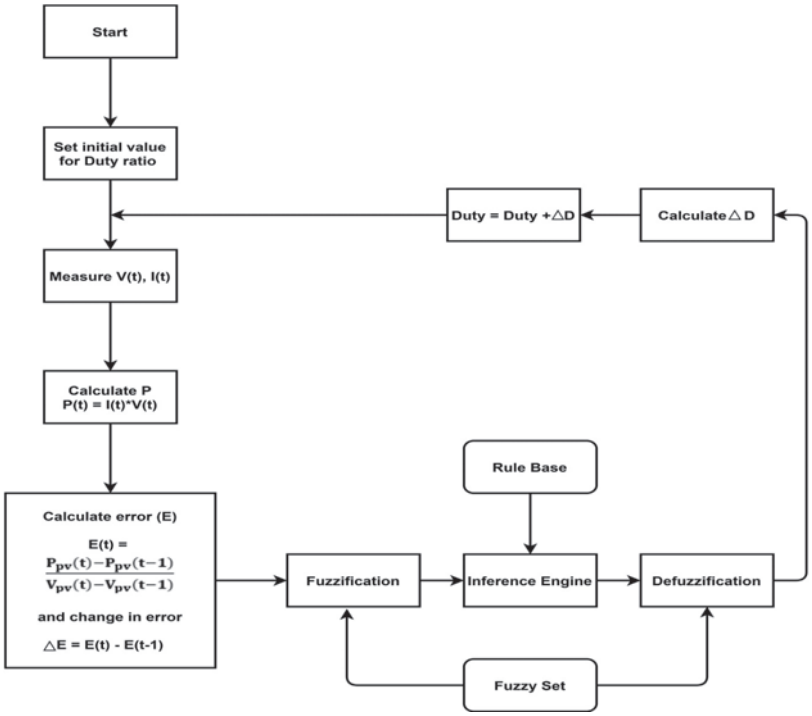

Figure 14 Flowchart of FLC MPPT.

Step VI: Calculate ΔE by subtracting E(t) with E(t–1), which is obtained from memory. This indicates the second input to the fuzzy logic controller.

Step VII: From the output of FLC incremental duty cycle is obtained which is later added to its previous value to obtain the final signal, which is later passed through the PWM generator to create switching pulses for the Boost Converter.

Figures 15 and 16 show the membership functions for the error and change in error respectively, whereas Figure 17 shows the membership function of the output. The surface view of the rule base designed for FLC based MPPT is shown in Figure 18.

3.4 Particle Swarm Optimization

Particle Swarm Optimization (PSO) based MPPT is particularly useful in situations which involve rapidly changing solar insolation levels, which can

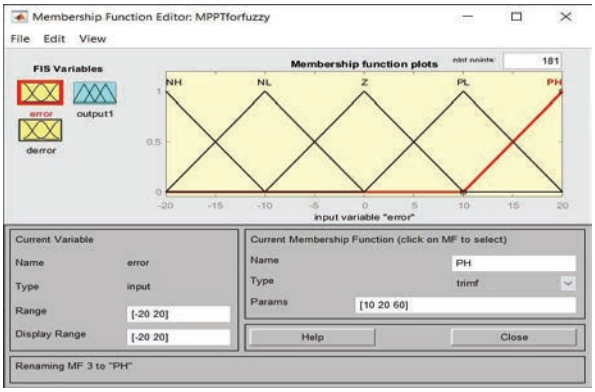

Figure 15 Membership function for error.

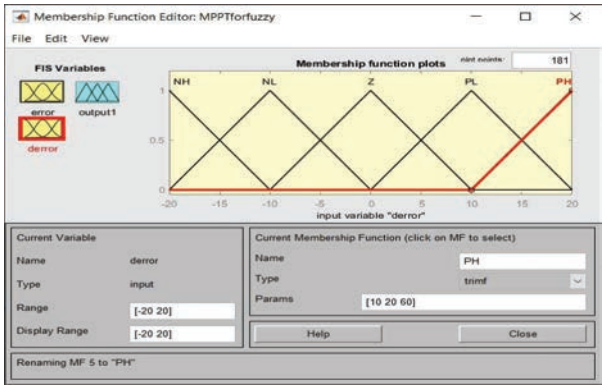

Figure 16 Membership function for change in error.

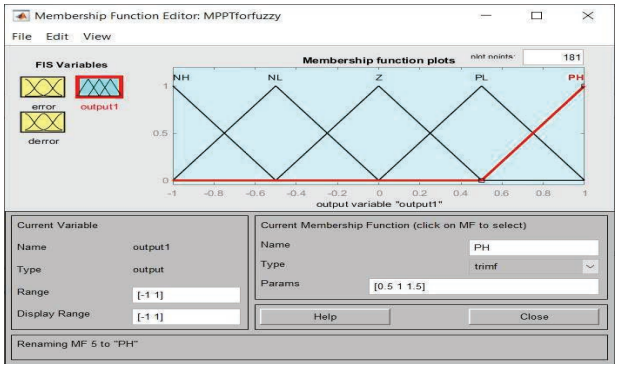

Figure 17 Membership function for output.

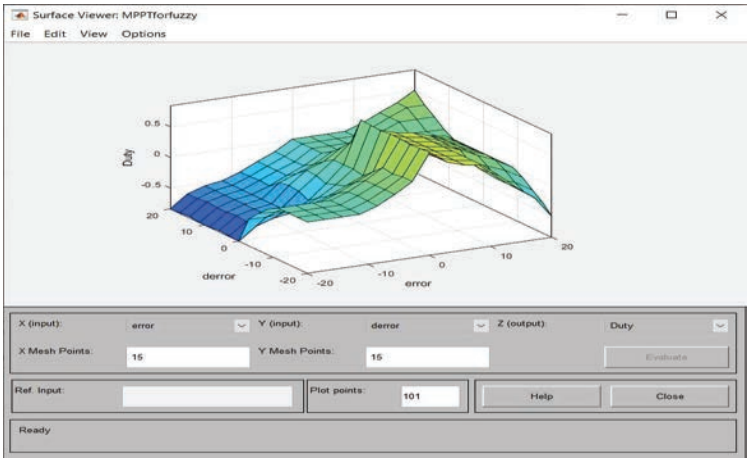

Figure 18 Surface view of fuzzy rules.

lead to ambiguous local values of MPP. In order to combat this problem, a number of particles are initialized in a multi-dimensional space, with position and velocity characteristics. Each such particle undergoes an optimization process that is mathematically performed by a fitness function. The best position of each individual particle, as well as the entire group is known to each particle. The particle movements are governed by the optimal position that suits the entire group. Here, a particle is represented by every instance of measured PV voltage. The equations governing the updating of velocity of position of particles are shown by Equations (12) and (13), and the pictorial representation of the movement of particles is shown in Figure 19.

$$v_i(m+1) = n \cdot v_i(m) + r_1 \cdot a_1 \cdot (p_{pi} - x_i(m)) + r_2 \cdot a_2 \cdot (p_{gl} - x_i(m)) \tag{12}$$

$$x_i(m+1) = x_i(m) + v_i(m+1) \tag{13}$$

Where

$i =$ optimization vector variable
$m =$ iteration number
$v_i(m) =$ velocity corresponding to i^{th} variable for m^{th} iteration
$x_i(m) =$ position corresponding to i^{th} variable for m^{th} iteration
r_1 and $r_2 =$ random numbers between 0 and 1
$n =$ inertia weight
a_1 and $a_2 =$ constants for algorithm's learning

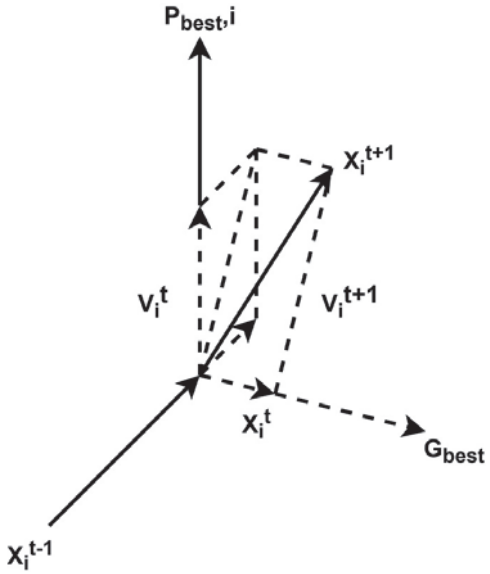

Figure 19 Movement of particles in the PSO algorithm.

p_{pi} = best local position for i^{th} particle
p_{gl} = best global position for all particles

Figure 20 shows the flowchart of the PSO MPPT algorithm. The stepwise execution of the algorithm in MATLAB is provided below.

Step I: Initialize the inputs as per Table 5.

Step II: Apply the objective function in order to determine the fitness of each particle, where fitness = I*PV (I, W, T). The objective function is chosen to be the output characteristic of the PV system during normal operating conditions and at a temperature of 25 degrees Celsius, as shown in Equation (14).

$$PV(I,W,T) = 1.1103log\frac{3.8W - I + 2.2 \times 10^{-8}}{2.2 \times 10^{-8}} - 0.2844I \qquad (14)$$

where

I = Photocurrent
W = Irradiance
T = Temperature

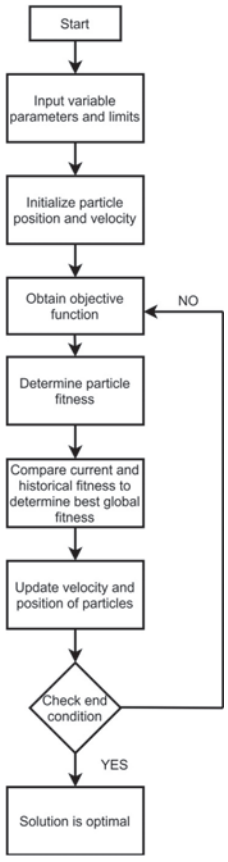

Figure 20 Particle Swarm Optimization MPPT algorithm.

Table 5 Initialization of parameters for PSO

Parameter	Specification
Maximum iterations	10
Inertia weight	0.8
Learning constants	2
Number of particles	10

Step III: Calculate the previous and new values of both the individual particle fitness and the global fitness.

Step IV: Based on the differences obtained in Step III, update the particle positions and velocities using Equations (12) and (13).

The velocity determining equation shown by Equation (12) consists of the following velocity components –

$n \cdot v_i(m) =$ particle intertia component
$r_1 \cdot a_1 \cdot (x_{pi} - x_i(m)) =$ local movement component
$r_2 \cdot a_2 \cdot (x_{gl} - x_i(m)) =$ group or global movement component.

These three components together describe the movement of the particles towards the global MPP.

Step V: Check whether the stopping condition is satisfied. The stopping condition is reached either when the number of iterations reaches its maximum possible limit, or if each of the particles are imparted a velocity by Equation (13) that is less than the minimum threshold.

3.5 Cuckoo Search Algorithm

The Cuckoo Search Algorithm (CSA) is based on the reproductive strategies utilized by the cuckoo birds. Cuckoo birds lay their eggs in the nests of other birds, and the process of searching of these nests follows a random walk, that is defined by the Levi flight function. They search an area with smaller steps for a nest, before jumping by a longer distance to the next area. A set of three rules that are followed for the searching process by Cuckoo birds is utilized for the purpose of optimization:

- A cuckoo bird lays a single egg at one instance, which is placed in a nest that is selected randomly.
- The nest with the highest quality of eggs survives.
- There is a fixed quantity of nests and the cuckoo's egg may or may not be discovered, i.e., the probability of discovery lies between 0 and 1.

The flowchart shown in Figure 21 gives an overview of the CSA. For the application of CSA for MPPT in PV systems, the various operating point voltages are considered as nests, with the fitness of each nest being calculated in terms of its power. If the worst nest is destroyed, it is replaced by a newly generated random nest, witht the global fitness values being iterated to update the global best nest. A new generation of cuckoos is introduced using the Levy flight function, with the global best nest being updated again. The criteria for stopping is considered to be the convergence of the global best nests.

The stepwise process for implementation of the CSA is mentioned below.

Step I: Initialize parameters for the CSA as per Table 6.

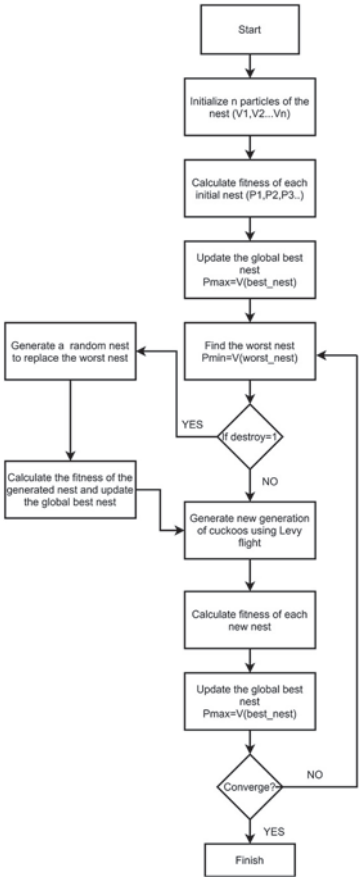

Figure 21 Cuckoo search algorithm MPPT.

Table 6 Initialization of parameters for CSA

Parameter	Specification
Maximum iterations	100
Number of nests	25
Probability of egg discovery by host	0.25

Step II: The fitness value of power is found as $P_{pv} = V_{pv} * I_{pv}$

Step III: Determine best value of current, and generate a random walk using the Levy flight function, as shown in Equation (15).

$$V_p{}^{(t+1)} = V_p{}^t + \alpha * Levy(\lambda) \tag{15}$$

where

$V_p^{(t+1)}$ = new solution for a cuckoo t
α = step size
$\text{Levy}(\lambda)$ = Levy flight function for generating random walk

Step IV: Fitness values are calculated for the new solutions that are obtained using Step III. These fitness values are then compared in order to obtain the best current, with multiple iterations of the nests (operating point voltages) being performed in order to obtain the MPP.

4 Results and Discussion

The performance of different MPPT algorithms is analyzed under a solar insolation curve as shown in Figure 22, which undergoes quick changes in irradiation levels. Figures 23, 24, 25, 26 and 27 shows the comparison between the PV power and the power obtained using MPPT for each of the five algorithms.

Figures 28, 29, 30, 31 and 32 shows the ratio between the output power and the input power for different MPPT algorithms. The performance of the intelligent MPPT technique (Fuzzy Logic Control) results in much lesser oscillation around the MPP when compared to the classical techniques (P&O and IC), due to the presence of multiple local MPPs and only one global MPP. Large variations in the ratio can especially be observed during the instances of rapid insolation change in case of P&O MPPT due to the algorithm undergoing confusion when tracking the global MPP, and resulting in drifting. Optimized techniques such as PSO and CSA based MPPT algorithms

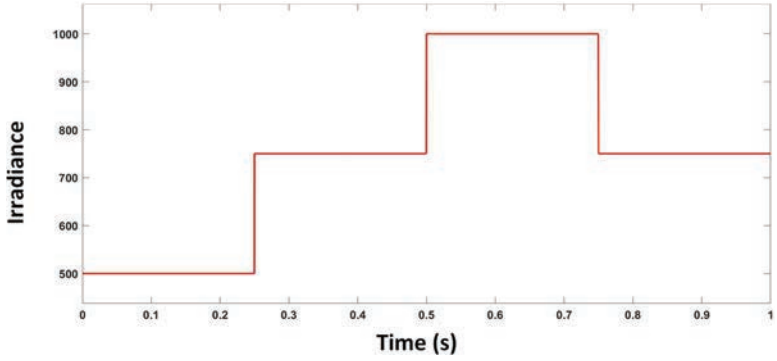

Figure 22 Irradiance profile.

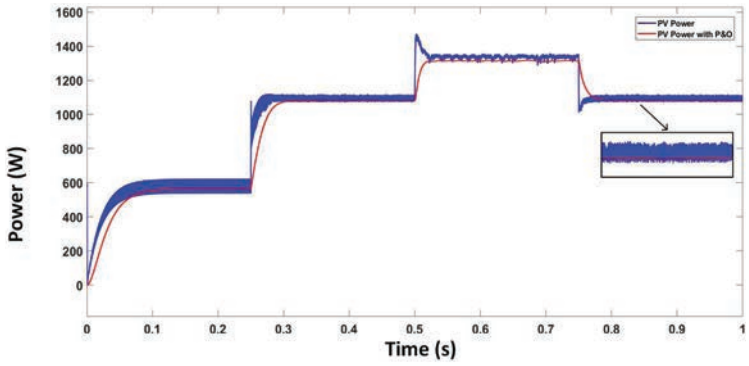

Figure 23 Comparison between PV power and MPPT power for P&O.

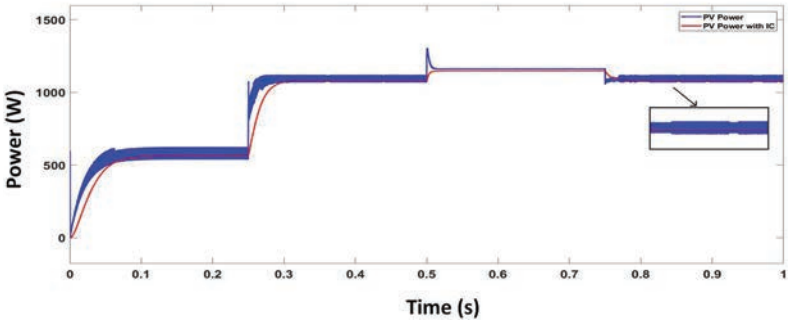

Figure 24 Comparison between PV power and MPPT power for IC.

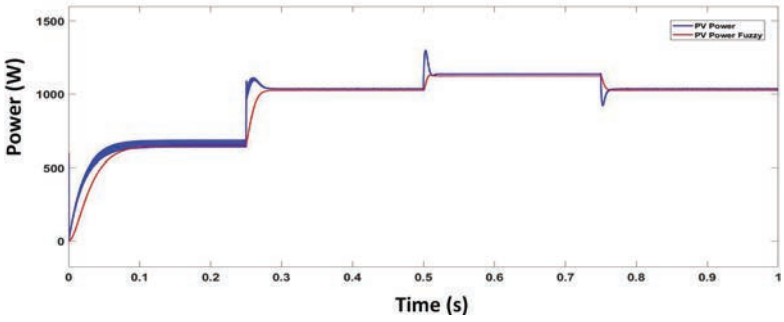

Figure 25 Comparison between PV power and MPPT power for Fuzzy.

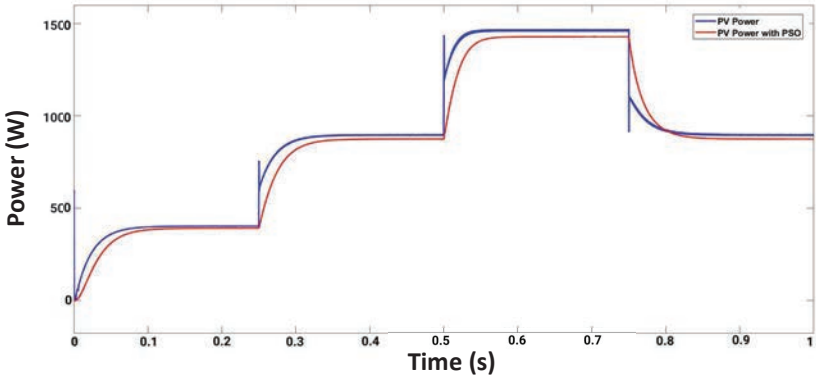

Figure 26 Comparison between PV power and MPPT power for PSO.

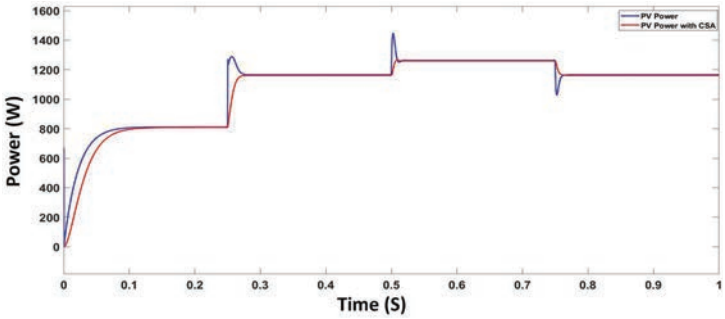

Figure 27 Comparison between PV power and MPPT power for CSA.

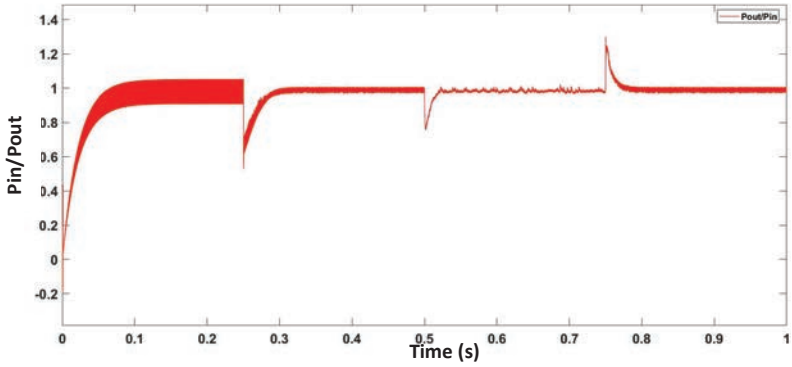

Figure 28 Ratio between output power and input power for P&O.

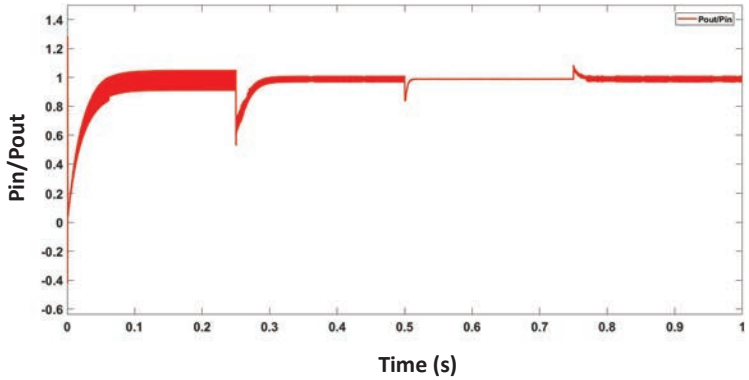

Figure 29 Ratio between output power and input power for IC.

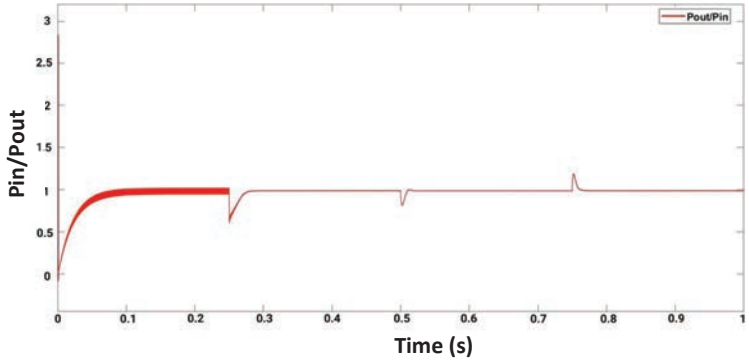

Figure 30 Ratio between output power and input power for FLC.

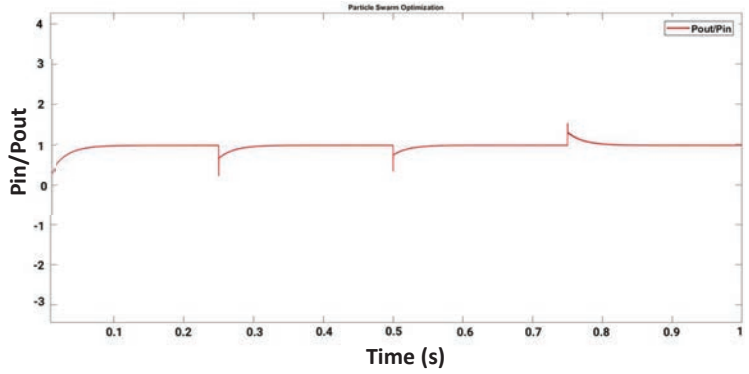

Figure 31 Ratio between output power and input power for PSO.

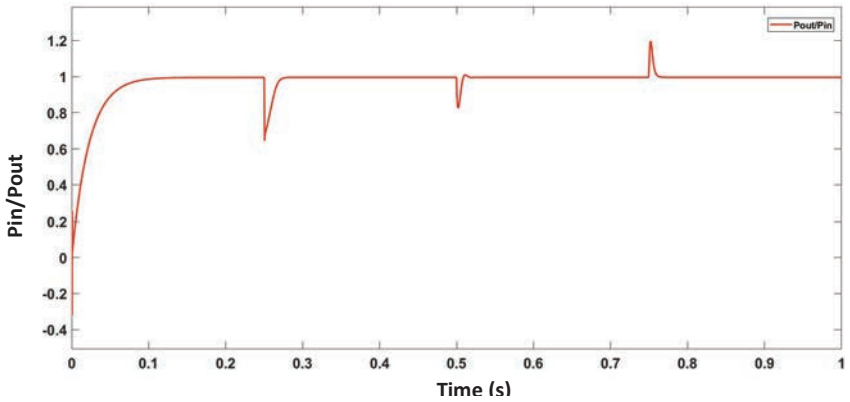

Figure 32 Ratio between output power and input power for CSA.

Table 7 Efficiencies for MPPT algorithms

Irradiance (W/m^2)		1000	750	500
PV Power (W)		1467.72	1031.46	586.57
P&O	**MPPT Power (W)**	1335.63	924.81	525.39
	Efficiency	91.01%	89.66%	89.57%
IC	**MPPT Power (W)**	1436.16	990.40	555.36
	Efficiency	97.85%	96.02%	94.68%
Fuzzy Logic	**MPPT Power (W)**	1449.96	1008.66	577.71
	Efficiency	98.79	97.79	98.49
PSO	**MPPT Power (W)**	1452.75	1018.15	573.61
	Efficiency	98.98%	98.71%	97.79%
CSA	**MPPT Power (W)**	1456.42	1018.98	586.57
	Efficiency	99.23%	98.79%	98.67%

$$\text{Efficiency} = \frac{\text{PV Power}}{\text{MPPT Power}}$$

result in even smoother waveforms, highlighting superior performance while tracking rapidly changing MPPs when compared to classical and intelligent techniques.

Table 7 highlights the efficiencies of the different MPPT algorithms under various insolation levels. The efficiency is calculated as the ratio of the PV power and that delivered by the MPPT algorithm. It is observed that CSA and PSO provide the highest efficiency for different irradiances, followed by FLC, IC and P&O algorithms. The large deviations in case of the MPP with P&O can be seen here. The applications of evolutionary optimization techniques

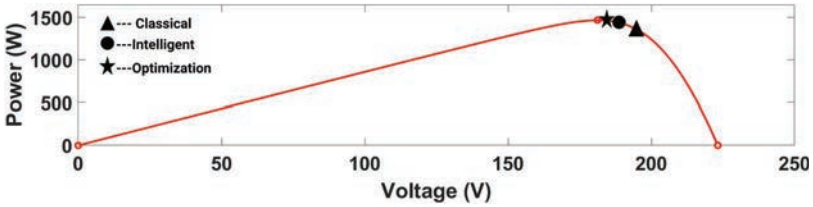

Figure 33 MPP for various algorithm categories for irradiance of 1000 W/m^2.

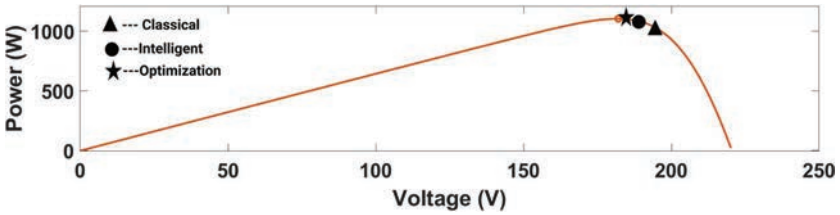

Figure 34 MPP for various algorithm categories for irradiance of 750 W/m^2.

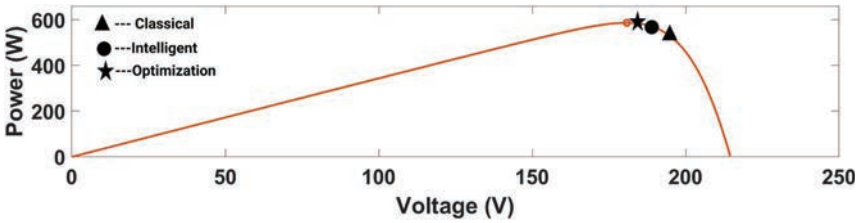

Figure 35 MPP for various algorithm categories for irradiance of 500 W/m^2.

for the process of MPPT is seen to clearly result in higher efficiencies, as in case of the PSO and CSA algorithms.

Figures 33, 34 and 35 are analytical representation of the performance of the three different algorithm categories during points of insolation change, based on the results form Table 7. The phenomenon of drifting of the MPP in case of classical MPPT(P&O) is clearly showcased. Among the classical MPPT algorithms, P&O functions on the basis of the deviations of the power, and when there is a rapid change in the solar insolation, the operating point also shifts to a higher point. In such a situation, the deviations in power are seen as positive, which tricks the MPPT algorithm into shifting away from the actual MPP. This drifting is mitigated by the IC algorithm, which is a modified classical technique, but comes with an inherent disadvantage of added complexity, since it requires two sensors to measure current and voltage.

This phenomenon of drifting is completely mitigated by the application of intelligent and optimization-based algorithms.

5 Conclusion

MPPT techniques are needed in order to ensure the maximum operation efficiency of standalone as well as grid-connected PV systems. In this paper, five different MPPT algorithms are surveyed and investigated – Perturb and Observe, Incremental Conductance, Fuzzy Logic, Particle Swarm Optimization and Cuckoo Search Algorithm. Comparisons are drawn between the PV power and the power delivered by the MPPT system in case of each of the algorithms under variable solar insolation, and their operational efficiencies calculated, with the CSA and PSO MPPT outperforming Fuzzy Logic, IC and P&O techniques. The oscillations around the MPP are observed in case of the classical (P&O and IC) algorithms, and the mitigation of the same by the intelligent (fuzzy logic) and optimization (PSO and CSA) algorithms is highlighted. The effect of drifting of the MPP that takes place for the classical techniques is also observed and highlighted, with the MPPs for the intelligent and optimization algorithms appearing to be much closer to the theoretical MPP.

References

[1] Kishore, V. V. N., ed. Renewable energy engineering and technology: principles and practice. The Energy and Resources Institute (TERI), 2010.
[2] Twidell, John, and Tony Weir. Renewable energy resources. Routledge, 2015.
[3] Faranda, Roberto, and Sonia Leva. "Energy comparison of MPPT techniques for PV Systems." WSEAS transactions on power systems 3.6 (2008): 446–455.
[4] Bataineh, Khaled. "Improved hybrid algorithms-based MPPT algorithm for PV system operating under severe weather conditions." IET Power Electronics 12.4 (2019): 703–711.
[5] Abdel-Salam, Mazen, Mohamed-Tharwat El-Mohandes, and Mohamed Goda. "An improved perturb-and-observe based MPPT method for PV systems under varying irradiation levels." Solar Energy 171 (2018): 547–561.

[6] Kamran, Muhammad, et al. "Implementation of improved Perturb & Observe MPPT technique with confined search space for standalone photovoltaic system." Journal of King Saud University-Engineering Sciences 32.7 (2020): 432–441.

[7] Alik, Rozana, and Awang Jusoh. "Modified Perturb and Observe (P&O) with checking algorithm under various solar irradiation." Solar Energy 148 (2017): 128–139.

[8] Ali, Ahmed IM, Mahmoud A. Sayed, and Essam EM Mohamed. "Modified efficient perturb and observe maximum power point tracking technique for grid-tied PV system." International Journal of Electrical Power & Energy Systems 99 (2018): 192–202.

[9] Shang, Liqun, Hangchen Guo, and Weiwei Zhu. "An improved MPPT control strategy based on incremental conductance algorithm." Protection and Control of Modern Power Systems 5.1 (2020): 1–8.

[10] Feroz Mirza, Adeel, et al. "Advanced variable step size incremental conductance MPPT for a standalone PV system utilizing a GA-tuned PID controller." Energies 13.16 (2020): 4153.

[11] Owusu-Nyarko, Isaac, et al. "Modified variable step-size incremental conductance MPPT technique for photovoltaic systems." Electronics 10.19 (2021): 2331.

[12] Motahhir, Saad, et al. "Modeling of photovoltaic system with modified incremental conductance algorithm for fast changes of irradiance." International Journal of Photoenergy 2018 (2018).

[13] Engel, Ekaterina A., and Nikita E. Engel. "Photovoltaic system control model on the basis of a modified fuzzy neural net." International Conference on Neuroinformatics. Springer, Cham, 2019.

[14] Nabipour, M., et al. "A new MPPT scheme based on a novel fuzzy approach." Renewable and Sustainable Energy Reviews 74 (2017): 1147–1169.

[15] Talbi, Billel, et al. "Design and hardware validation of modified P&O algorithm by fuzzy logic approach based on model predictive control for MPPT of PV systems." Journal of Renewable and Sustainable Energy 9.4 (2017): 043503.

[16] Bouakkaz, Mohammed Salah, et al. "Fuzzy logic based adaptive step hill climbing MPPT algorithm for PV energy generation systems." 2020 International Conference on Computing and Information Technology (ICCIT-1441). IEEE, 2020.

[17] Cheng, Po-Chen, et al. “Optimization of a fuzzy-logic-control-based MPPT algorithm using the particle swarm optimization technique.” Energies 8.6 (2015): 5338–5360.
[18] Li, Hong, et al. “An overall distribution particle swarm optimization MPPT algorithm for photovoltaic system under partial shading.” IEEE Transactions on Industrial Electronics 66.1 (2018): 265–275.
[19] Yoganandini, A. P., and G. S. Anitha. “A modified particle swarm optimization algorithm to enhance MPPT in the PV array.” International Journal of Electrical and Computer Engineering 10.5 (2020): 5001.
[20] Mao, Mingxuan, et al. “A two-stage particle swarm optimization algorithm for MPPT of partially shaded PV arrays.” International Journal of Green Energy 14.8 (2017): 694–702.
[21] Nugraha, Dimas Aji, and Kuo-Lung Lian. “A novel MPPT method based on cuckoo search algorithm and golden section search algorithm for partially shaded PV system.” Canadian Journal of Electrical and Computer Engineering 42.3 (2019): 173–182.
[22] Basha, CH Hussaian, et al. “Development of cuckoo search MPPT algorithm for partially shaded solar PV SEPIC converter.” Soft Computing for Problem Solving. Springer, Singapore, 2020. 727–736.
[23] Mosaad, Mohamed I., et al. “Maximum power point tracking of PV system based cuckoo search algorithm; review and comparison.” Energy Procedia 162 (2019): 117–126.

Biographies

Aditya Ghatak is currently pursuing his bachelor’s degree in electrical and electronics engineering from Vellore Institute of Technology, India, His research interest includes power systems, renewable energy systems and electric vehicles.

Tushar Pandit is currently pursuing a bachelor's degree in Electrical and Electronics Engineering from Vellore Institute of Technology, India. His interests lie in power systems, renewable resources, distributed generation and microgrids, electric vehicles, and smart energy.

Dharavath Kishan received the B. Tech degree in Electrical and Electronics Engineering and M. Tech degree in Power Electronics from Jawaharlal Nehru Technological University Hyderabad respectively in 2011 and 2013 and he received his PhD degree from National Institute of Technology Tiruchirappalli in 2018. Currently he is working as Assistant Professor in Department of E & E Engineering at National Institute of Technology Karnataka (NITK), Surathkal, India. Prior to joining NITK he worked as Assistant Professor at Faculty of Science and Technology, IFHE Hyderabad. Dr Kishan current research interests include power electronics and its applications in electric vehicles, wireless power transfer and transportation electrification. He has published 16 research papers in reputed journals and peer reviewed international conferences. He is also delivered guest lectures at various events on Wireless Power Transfer for electric vehicles. He is also an IEEE Senior Member and IAS, PELS & IES Society member. Dr Kishan is also an active reviewer for various reputed IEEE transactions like IEEE Transactions on Electromagnetic compatibility, IEEE Transactions on Industrial Electronics,

IEEE Transactions on vehicular Technology, and IEEE Access, IET Renewable Power Generation. He has guided two master level students in the area of power electronics and currently guiding one master and Five PhD students in the area of Power Electronic Applications.

Ravi Raushan received the B. Tech degree in Electrical Engineering and M. Tech degree in Mechatronics from Maulana Abul Kalam Azad University of Technology, Kolkata respectively in 2010 and 2012. He received his PhD degree from Indian Institute of Technology (Indian School of Mines) Dhanbad in 2018. Currently he is working as Assistant Professor in Department of E & E Engineering at National Institute of Technology Karnataka (NITK), Surathkal, India. His research interests are power electronic converters and its application in renewable energy.